



Contents lists available at ScienceDirect

## Chinese Herbal Medicines

journal homepage: [www.elsevier.com/locate/chmed](http://www.elsevier.com/locate/chmed)

## Original Article

Metabolomics investigation on antiobesity effects of *Corydalis bungeana* on high-fat high-sugar diet-induced obese ratsMinghai Fu<sup>a,b</sup>, Terigele Bao<sup>b</sup>, Hongzhen Yu<sup>b</sup>, LiSha A.<sup>a</sup>, HuiFang Li<sup>b</sup>, Genna Ba<sup>b</sup>, Sungbo Cho<sup>a,b,\*</sup><sup>a</sup> Key Laboratory of Tropical Translational Medicine of Ministry of Education, Hainan Key Laboratory for Research and Development of Tropical Herbs, School of Pharmacy, Hainan Medical University, Haikou 571199, China<sup>b</sup> NMPA Key Laboratory of Quality Control of Traditional Chinese Medicine (Mongolian Medicine), Inner Mongolia Minzu University, Tongliao 028000, China

## ARTICLE INFO

## Article history:

Received 20 December 2021

Revised 24 February 2022

Accepted 6 April 2022

Available online 6 July 2022

## Keywords:

*Corydalis bungeana* Turcz.

GC-TOF/MS

metabolomics

Mongolian medicine

obesity

## ABSTRACT

**Objective:** *Corydalis bungeana* (CB) is a well-used medicinal herb in Mongolian folk medicine and has been traditionally applied as an antiobesity agent. However, the evidence-based pharmacological effects of CB and its specific metabolic alterations in the obese model are not entirely understood. This study aimed to utilize untargeted metabolomic techniques to identify biomarkers and gain mechanistic insight into the serum metabolite alterations associated with weight loss and lipid metabolism in obese rats.

**Methods:** A high-fat high-sugar (HFHS) diet was used to induce obese models in rats. CB extract was orally gavaged at 0.18, 0.9 and 1.8 g/kg doses for six weeks, and feed intake, body weight, fat pad weight, and blood indexes were measured. Blood serum metabolites were evaluated by gas chromatography/quadrupole time-of-flight tandem mass spectrometry (GC-TOF/MS).

**Results:** The results showed that compared with the obese group, the administration of CB extract caused significant decreases in body weight ( $P < 0.05$ ), feed intake, Lee's index, and perirenal, mesenteric, epididymal fat weight. CB extract also reduced blood triglyceride and total cholesterol levels ( $P < 0.05$ ) of obese rats. Metabolomic findings showed that nine differential metabolites, including pyruvic acid, D-glucuronic acid, malic acid, dimethylglycine, oxoglutaric acid, pantothenic acid, sorbitol acid, fumaric acid and glucose 6-phosphate were identified under CB treatment and altered metabolic pathways such as TCA cycle, pantothenate and CoA biosynthesis, and glycolysis/gluconeogenesis.

**Conclusion:** This study demonstrated weight loss and lipid lowering effects of CB on HFHS diet-induced obese rats and identified nine metabolites as potential biomarkers for evaluating the favorable therapeutic mechanism of CB via regulation of lipid and glucose metabolism.

© 2022 Tianjin Press of Chinese Herbal Medicines. Published by ELSEVIER B.V. This is an open access article under the CC BY-NC-ND license (<http://creativecommons.org/licenses/by-nc-nd/4.0/>).

## 1. Introduction

Obesity is a significant risk factor for metabolic syndrome and is characterized as an excessive accumulation of adipose tissues in the body (O'Neill & O'Driscoll, 2015). Studies reported that chronic over-consumption of carbohydrates or fat causes deposition in visceral adipose organs such as perirenal, mesenteric, and epididymal adipose tissues (Liu et al., 2020). Metabolically unhealthy obese persons have an abnormal adipose tissue function, more ectopic fat storage, and less insulin sensitivity than healthy individuals (Aung et al., 2014). Pharmacologically active compounds such as orlistat, lorcaserin, phentermine, and topiramate treat obesity by altering the rate of metabolism (Cataldi et al., 2019). How-

ever, these drugs have multiple side effects, including gastrointestinal discomfort, diarrhea, insomnia, stroke, suicidal tendency, and depression (Bessesen & Van, 2018). Many natural ingredients (e.g. caffeine and linarin) have shown the potential to counteract obesity (Dangol et al., 2017; Wang et al., 2021). Therefore, traditional medicinal herbs might be a better alternative to combat obesity without adverse effects.

Dried whole herb *Corydalis bungeana* Turcz. (CB) is one key component of Digda Mongolian traditional medicine, which includes around 20 species of different medicinal plants and is frequently used in many prescriptions. As a word originated from the Sanskrit language, Digda means extremely bitter. In Mongolian medicine, it has been recorded that CB can be used as an antiobesity agent (Ba & Li, 2012). Current bitter taste receptor in physiological studies also reveals the regulatory effects of bitter compounds on hunger-satiety cycle and fat oxidation (Venables

\* Corresponding author.

E-mail address: [blue0555@hotmail.com](mailto:blue0555@hotmail.com) (S. Cho).

et al., 2008; Shafaie et al., 2013). In addition, CB has long been used in traditional medicine to prevent other diseases such as hordolum, icteric hepatitis, and hemorrhoids (Tian et al., 2019; Zhai et al., 2016; Dong et al., 2015). Alkaloids, steroids, and flavonoid glycosides are main active compounds extracted and identified from CB with various biological effects, including antibacterial activity, anti-inflammatory, and immune regulatory functions (Gao et al., 2018; Dong et al., 2018; Yang et al., 2016). However, the antiobesity and fat metabolism effects of CB have not been well investigated.

Metabolomics is a widely employed and high-throughput analytical methodology to identify biomarkers, reveal pathways, and illustrate mechanisms of metabolic diseases (Bao et al., 2020). Several studies have proven that gas chromatography/quadrupole-time-of-flight tandem mass spectrometry (GC-TOF/MS) based metabolomics is a powerful tool for comprehensively profiling the metabolic process of adiposity (Mesnage et al., 2018; Darcy et al., 2020; Hu et al., 2020). Hence, this study aimed to investigate the antiobesity effect and fat metabolic mechanisms of CB on HFHS diet-induced obese rats through evaluation of biochemical and histological assays, metabolic changes, and metabolic pathway analyses. GC-TOF/MS-based metabolomics approaches were used to provide comprehensive serum metabolites in untargeted metabolomics analysis.

## 2. Materials and methods

### 2.1. Materials

The whole plant of CB was collected from Xilinhaote, Inner Mongolia, China. Blood hormone kits were purchased from Nanjing Jiancheng Bioengineering Institute (Nanjing, China). Methoxyamine HCl, fatty acid methyl ester (C7–C30, FAMES) standards, pyridine, and anhydrous sodium sulfate were obtained from Sigma-Aldrich (St. Louis, USA). *N*-methyl-*N*-(trimethylsilyl)trifluoroacetamide with 1% (volume percentage) trimethylchlorosilane (MSTFA, with 1% TMCS), methanol (Optima LC-MS), acetonitrile (Optima LC-MS), hexane, dichloromethane, chloroform, and acetone were purchased from Thermo-Fisher Scientific (Fairlawn, New Jersey, USA). Ultrapure water was produced by a Mill-Q Reference system equipped with an LC-MS Pak filter (Millipore, Billerica, MA).

### 2.2. Animals and experimental design

Six to eight weeks old male Wistar rats (initial body weight =  $220 \pm 10$  g) were obtained from Changsheng Biotechnology Co., Ltd (Shenyang, China). All rats were individually housed in a temperature-controlled room with a 14–10 h light–dark cycle and allowed 7 d for acclimatization (20–25 °C) and *ad-libitum* access to water. Obesity was induced using a high-fat high-sugar diet (25% lard oil, 20% sugar, and 55% regular diet) for 10 weeks, while the control group was given a regular diet as previously described (Deng et al., 2016; Xu et al., 2020). Body weight and food intake were recorded weekly. Obese animals were randomly allocated to one of the five experimental groups and oral gavage with Orlistat at 0.03 g/kg and CB extracts at 0.18 g/kg, 0.9 g/kg, and 1.8 g/kg doses for six weeks. At the end of the experimental day, animals' body lengths were measured for Lee's index and anesthetized with 50 mg/kg pentobarbital sodium. Blood was collected from the abdominal aorta and centrifuged at 4500 r/min for 10 min at 4 °C. The supernatant was collected and stored at –80 °C. Liver, mesenteric adipose tissue, perirenal adipose tissue, and epididymal adipose tissue (fat pads) were surgically isolated from each rat, freed from surrounding tissues, and wet weights were measured. All experiments were performed following protocols reviewed

and approved by the Institutional Animal Care and Use Committee, Inner Mongolian University for Nationalities (approval number: NM-LL-2021-06-15-1).

### 2.3. Serum TC and TG analysis

An automatic biochemical analyzer (C-311, Roche, China) was used to estimate the levels of total cholesterol (TC) and triglyceride (TG) following the manufacturer's instructions. A total of 100  $\mu$ L serum was used for the test, and the absorbance was measured at 450 nm.

### 2.4. H&E staining

The perirenal adipose tissue, epididymal adipose tissue, and mesenteric adipose tissue samples were fixed with 4% formalin and processed to generate 3–5  $\mu$ m thick paraffin sections. The sections were stained with hematoxylin and eosin (H&E) before being examined under an Olympus microscope equipped with a CCD camera (Nikon DS-U3, Japan). An image analysis software system (Nikon Eclipse E100, Japan) was used for microscopic examination at  $\times 400$  magnification.

### 2.5. Metabolomic analysis

#### 2.5.1. Sample preparation

The metabolite extraction was carried out immediately after thawing the samples on ice. Firstly, the metabolite extracts were lyophilized to dry powder using a Free Zone freeze dryer (Labconco, Kansas City, MO, USA) after removing chloroform in a CentriVap vacuum concentrator (Labconco, Kansas City, MO, USA). The 50 mg frozen samples harvested and stored in a microcentrifuge tube were mixed with 25 mg of pre-chilled zirconium oxide beads and 10  $\mu$ L of internal standards. Each aliquot of 50  $\mu$ L of 50% pre-chilled methanol was added for automated homogenization. After centrifugation at 14 000 g and 4 °C for 20 min (Microfuge 20R, USA), the supernatant was carefully transferred to an autosampler vial (Agilent Technologies, Foster City, CA, USA), evaporated briefly to remove chloroform in a CentriVap vacuum concentrator, and further lyophilized using a Free Zone freeze dryer. The rest of the samples were pooled for the quality control samples. The dried sample was derivatized with 50  $\mu$ L of methoxyamine (20 mg/mL in pyridine) at 30 °C for 2 h, followed by addition of 50  $\mu$ L of MSTFA (1% TMCS) containing FAMES as retention indices at 37.5 °C for 1 h.

#### 2.5.2. GC-TOF/MS conditions

The sample analysis was conducted by a time-of-flight spectrometry (GC-TOF/MS) system (Pegasus HT, Leco Corp., St. Joseph, MO, USA) with an Agilent 7890B gas chromatography and a Gerstel multipurpose sample MPS2 with dual heads (Gerstel, Germany). The separation was carried out on a Rxi-5 ms capillary column (30 m  $\times$  250  $\mu$ m i.d., 0.25- $\mu$ m film thickness; Restek corporation, Bellefonte, PA, USA). The sample injection volume was 1.0  $\mu$ L and Helium was used as the carrier gas at a constant flow rate of 1.0 mL/min. The temperature of injection and transfer interface were both maintained at 270 °C and the source temperature was 220 °C. The data acquisition rate was set at 25 spectra/s. The measurement were made using electron impact ionization (70 eV) in the full scan mode ( $m/z$  50–550 Da).

#### 2.5.3. Data analysis

The original data generated by GC-TOF/MS were automatically exported to XploreMET (Metabo-Profile Biotechnology, Shanghai, China) through ChromaTOF software for automated baseline denoising and smoothing, peak picking and deconvolution, creating reference database from the pooled QC samples, metabolite

signal alignment, missing value correction and imputation, metabolite identification as well as data preprocessing (normalization and standardization). Then, all data were converted into comparable data vectors for statistical analysis. Each value was mean-centered and scaled by the standard deviation of the experimental measurements. Principal component analysis (PCA) and orthogonal partial least-square discriminant analysis (OPLS-DA) were performed by XplormET software. The value of variable importance in the projection (VIP) was used to weight the sum of squares of the PLS weights. The metabolic pathway of differential metabolites was investigated in the Kyoto Encyclopedia of Genes and Genomes (KEGG).

## 2.6. Statistical analysis

Data are presented as mean  $\pm$  standard error of the mean. The statistical analyses were performed using GraphPad prism 7.04. Data were analyzed by One-way ANOVA. Treatment differences were analyzed by the Tukey Test. Results were considered significant at  $P < 0.05$ . Metabolites were considered statistically significant if a variable is  $VIP \geq 1.5$  and  $P < 0.05$ .

## 3. Results

### 3.1. CB extract reduced feed intake and body weight of HFHS diet-induced obese rats

To evaluate whether CB could prevent HFHS diet-induced obesity, CB extract (0.18, 0.9, and 1.8 g/kg) were orally gavaged to HFHS rats for six weeks. We found that body weight and Lee's index were significantly increased in HFHS groups compared to control rats ( $P < 0.05$ ), while feed intake was markedly decreased in HFHS groups. The administration of CB extracts caused significant decreases in body weight ( $P < 0.05$ ), feed intake ( $P < 0.01$ ) and Lee's index ( $P < 0.05$ ) in comparison with the obese group (Fig. 1).

### 3.2. Effect of CB extract on serum TC and TG levels

As shown in Fig. 2, the serum level of TC and TG were significantly elevated in the HFHS group compared to the control group. Compared to the HFHS group, TC and TG serum levels were significantly decreased in three different doses of CB extract groups ( $P < 0.05$ , 0.01). As expected, positive medication such as orlistat also considerably reduced serum TC and TG levels compared to the obese group ( $P < 0.05$ ).

### 3.3. CB extract suppresses lipid accumulation in HFHS diet-induced obese rats

As shown in Fig. 3, the HFHS diet significantly increased mesenteric, epididymal, and perirenal fat deposition than the control group. In contrast to the HFHS group, CB extract at 1.8 g/kg dose significantly decreased the relative weights of epididymal and perirenal fat tissues by 11.9% and 16.2% ( $P < 0.05$ ), respectively (Fig. 3A and B). Moreover, the relative mesenteric fat weight was significantly decreased by CB extract at three different doses by a maximum of 23.1% ( $P < 0.05$ ) (Fig. 3C). As expected, orlistat profoundly decreased mesenteric, epididymal, and perirenal fat deposition compared to the HFHS group ( $P < 0.05$ ). To assess the morphological changes in mesenteric, epididymal, and perirenal fat tissues, they were collected from the experimental animals and compared through HE staining. The results showed that many adipocytes in three types of adipose tissues were observed in the HFHS group, and the size of adipocytes was decreased in CB treatment groups compared to the HFHS group (Fig. 4).

### 3.4. Untargeted metabolomics study

#### 3.4.1. Data quality and identification of metabolites

Based on previous pharmacological findings, the therapeutic dose of CB at 1.8 g/kg group was selected for a GC-TOF/MS metabolomic analysis. A total of 160 metabolite annotations of different classes were detected in 18 serum samples using untargeted metabolomics analysis. These metabolites were fatty acids, nucleotide, lipids, amino acids, organic acids, carbohydrates, and others, among which amino acids, organic acids, and carbohydrates account for 33%, 20%, and 17%, respectively (Fig. 5A).

For subtle changes, a sophisticated multivariate analysis of individual metabolic profiles from each group was carried out. Firstly, principal component analysis (PCA) was based on these serum metabolites. A clear separation was observed among the groups, with 30.29% interpretation powers (Fig. 5B). Also, Orthogonal projections to latent structures discriminant analysis (OPLS-DA) revealed a distinguishable pattern between groups (Fig. 5I). These results suggested that CB supplementation dramatically altered the metabolic profiles in the serum of HFHS-fed rats.

#### 3.4.2. Changes of metabolites and biological metabolic pathways

We screened the differential metabolites in the serum among the groups with double criteria of variable importance for the projection (VIP)  $> 1.5$  and  $P < 0.05$  in multivariate and univariate statistical analyses simultaneously. A total of 31 and 17 differential metabolites and metabolite ratios were identified between control vs. HFHS and HFHS vs. CB-1.8, respectively (Table S1). The heat map summarizes expressed metabolic profiles of all the samples.

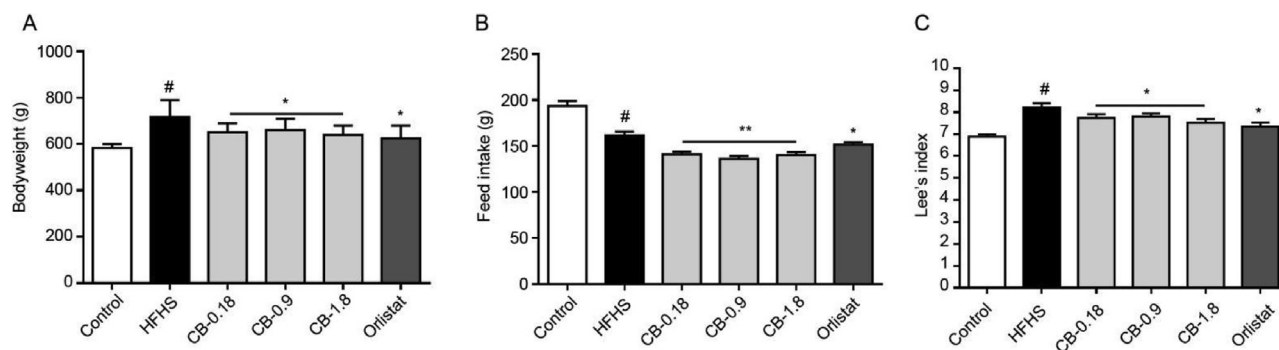


**Fig. 1.** CB extract reduced body weight (A), feed intake (B) and Lee's index (C) in HFHS diet-induced obese rats (mean  $\pm$  SEM,  $n = 10$ ). <sup>#</sup> $P < 0.05$  vs control group; <sup>\*</sup> $P < 0.05$  and <sup>\*\*</sup> $P < 0.01$  vs HFHS group.



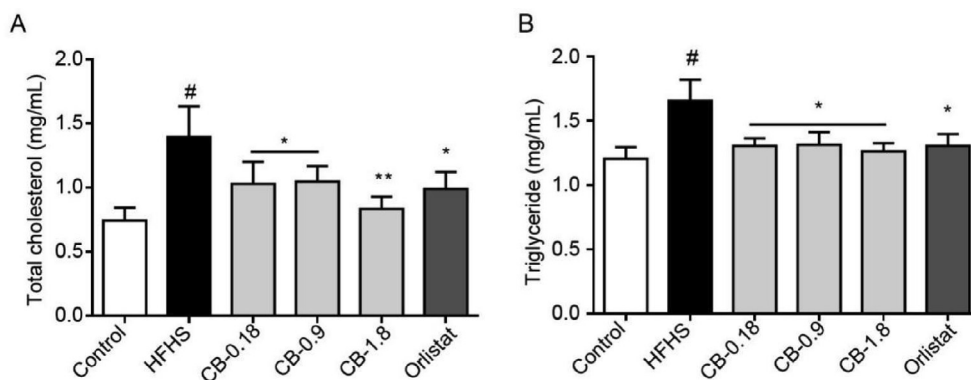


Fig. 2. Effects of CB extract on serum TC (A) and TG (B) levels (mean ± SEM, n = 10). #P < 0.05 vs control group; \*P < 0.05 and \*\*P < 0.01 vs HFHS group.

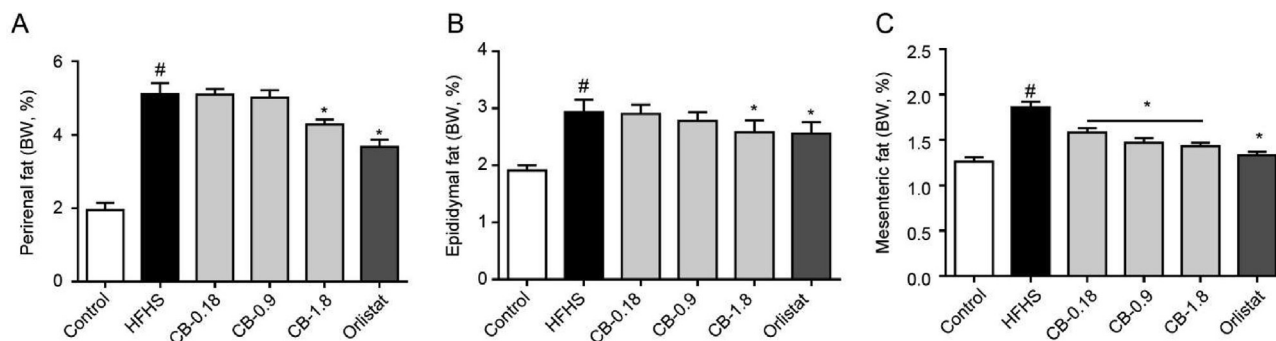


Fig. 3. CB extract suppresses relative weights of perirenal (A), epididymal (B), and mesenteric (C) fat depositions in HFHS rats (mean ± SEM, n = 10). #P < 0.05 vs control group; \*P < 0.05 and \*\*P < 0.01 vs HFHS group.

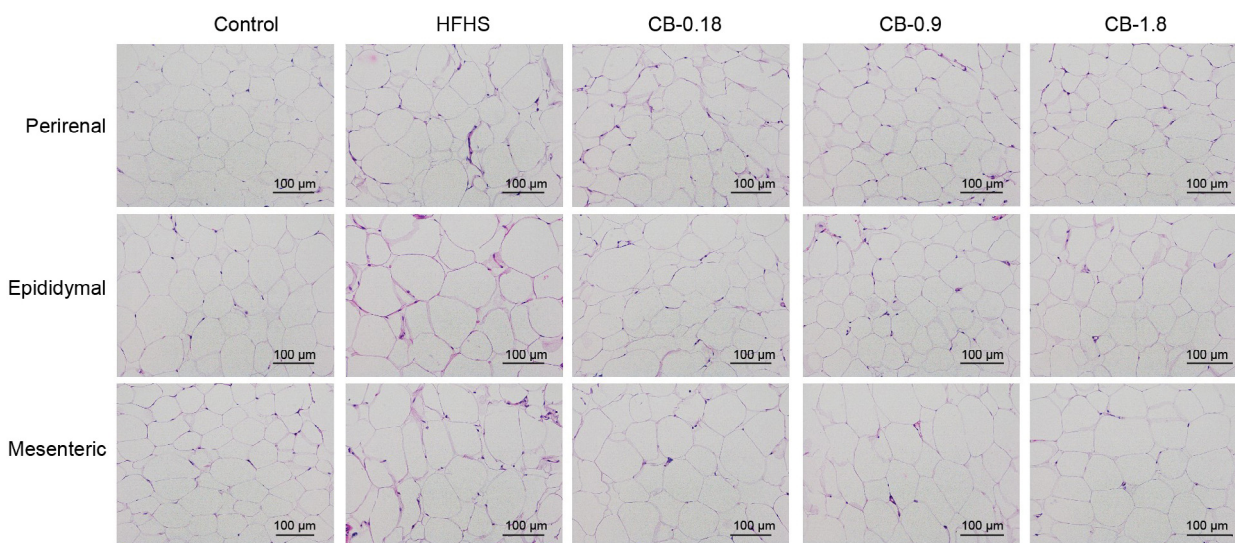


Fig. 4. Histological changes emerged from perirenal, epididymal and mesenteric fat tissues of five experimental groups of rats. H&E stained sections of fat tissues were observed with an optical microscope at ×400.

It presents considerable variability that existed in metabolomic-wide expression among the control, HFHS, and CB-1.8 groups (Fig. 5C).

The analysis of differential metabolites was carried out by using univariate statistical analysis (Student’s *t*-test). An enhanced volcano plot showed the differential metabolites selected with the multicriteria assessment between the HFHS and CB-1.8 (Fig. 6A) as well as the control and HFHS groups (Fig. S2). The right side

indicated increased metabolites in the CB group; the left indicated decreased metabolites compared to the HFHS group. Metabolic pathway analysis revealed 112 differential metabolites, and their ratio across the group was *P* value < 0.05 and VIP ≥ 1.5.

Between the HFHS and CB-1.8 groups, six were up-regulated, whereas one was down-regulated (Fig. 6B). From the KEGG pathway database, four pathways were showing significant changes after the treatment. The main altering pathways were citrate cycle

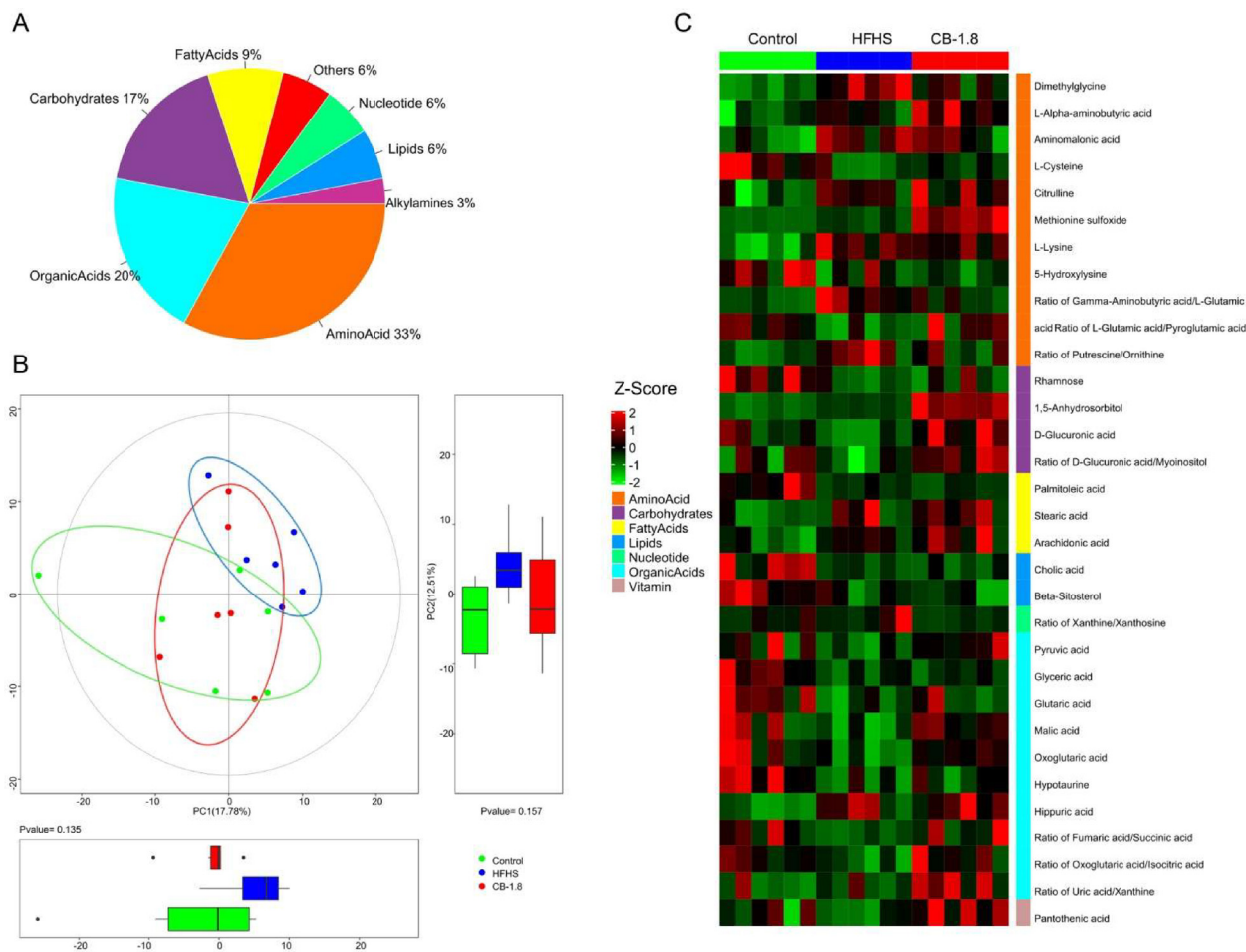


**Fig. 5.** Metabolite classes and compositions detected in samples. A: Pie chart indicating the abundance ratio of different chemical classes of annotated metabolites identified by untargeted metabolic profiling in serum samples. B: Overview of the serum metabolic profiles of three groups using a principal component analysis (PCA) scores plot and boxplot ( $n = 6$  per group). C: The differences in expression among the three groups of differential metabolites in serum were displayed heatmap. Red and green entries indicated metabolites that showed respectively more or fewer expressions in each sample.

(or tricarboxylic acid cycle, TCA cycle), glycine, serine and threonine metabolism, and *D*-glutamine and *D*-glutamate metabolism (Fig. 6C). The nine representative differential metabolites including fumaric acid, sorbitol, glucose 6-phosphate, pyruvic acid, *D*-glucuronic acid, malic acid, dimethylglycine, oxoglutaric acid, and pantothenic acid obtained from the key altered pathways were illustrated in Fig. 7A–I. The results showed that CB supplements could alter the metabolites in the HFHS group.

#### 4. Discussion

The current study investigated the anti-obesity and lipid lowering effects of CB extract on HFHS diet-induced obese rats. Obesity is a consequence of the high carbohydrate and lipid consumption (Bessesen & Van, 2018). HFHS diet could induce metabolic syndromes including glucose tolerance, insulin resistance, diabetes mellitus, hypertension, and hypertriglyceridemia in animal models (Sumiyoshi, Sakanaka, & Kimura, 2006; Stanhope et al., 2009; Yang et al., 2012). The HFHS diet is a suitable diet practice for investigating the anti-obesity effects in animals. In this study, the obese rats were induced by HFHS diet feeding for 10 weeks. Our results of developing obese model were highly consistent with previous observations (Deng et al., 2016; Amor et al., 2019; Xu et al., 2020). The obese group resulted in higher body weight than control group as well as higher perirenal, epididymal, and mesenteric

adipose tissues. The H&E staining results clearly showed the reduction of fat deposition. Also, the obese group showed increased levels of serum TG and TC, which indicating an increase in lipid metabolism shifting glucose to lipids (Zhang et al., 2008; Mooradian, 2009).

Metabolomics is a powerful tool for understanding the metabolic disorder and the therapeutic mechanisms of medicinal plants. In this study, using GC-TOF/MS analysis technique we carried out the metabolites profiling in serum to investigate the anti-obesity mechanism of CB extract. The metabolites in serum are capable to represent the overall condition of animals and reflect the metabolic abnormalities. The obese group showed higher levels of unsaturated fatty acids (FA) such as arachidonic, linoleic, oleic and stearic acids in serum compared to the control group. It is well-known that obesity disturbs the glycerolipid/free FA cycle (Prentki & Madiraju, 2012). The administration of CB extracts notably indicated lower serum TC and TG levels and reduced adipose tissue sizes. The lipid metabolism is closely interrelated glucose-energy metabolism, hence we carried out the metabolomic analysis to investigate the alteration of metabolites in glucose-energy metabolism.

In the metabolomic study, mainly three essential pathways, pantothenate and CoA biosynthesis, TCA cycle, glycolysis and gluconeogenesis pathways were involved in the anti-obesity effects of CB extract. The obese group showed down-regulated levels of

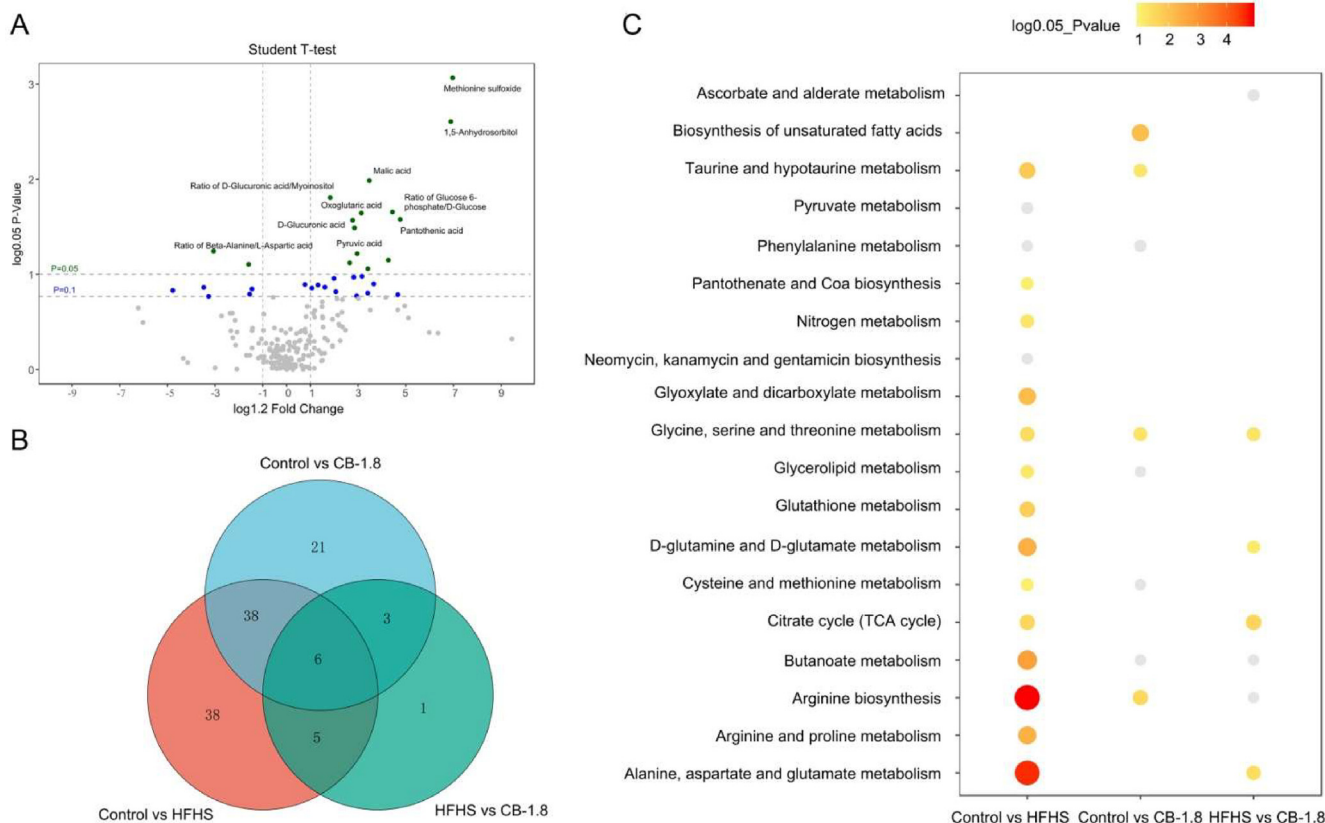


**Fig. 6.** Differential metabolites and pathways across groups. A: A volcano plot showed the differential metabolite profiles between the HFHS and CB-1.8 groups. B: Differential metabolites across the multiple group comparisons. C: The fold change is displayed with a cut-off value of green dot < 0.05, blue dot < 0.1 for P-value. C. XploreMET (Metabo-Profile) was used to analyze the metabolic pathways on the KEGG website of the differential metabolites.

fumaric acid, oxoglutaric acid, and pyruvic acid participated in TCA cycle, which is an essential metabolic pathway for glucose, amino and FAs. The altered metabolites between control and obese group explained the suppression of the glycolysis. HFHS diet is known to accelerate gluconeogenesis (Tang et al., 2018). In diabetic rats, high energy consumption can lead to lowering pyruvate and alanine levels by down-regulating the hexokinase, phosphofructokinase, and pyruvate kinase enzymes in glycolysis (Mediani et al., 2018). The pyruvate which is transformed from glucose was significantly decreased by glycolysis. Thus, the model group showed the disturbance of the energy and glucose homeostasis. On the other hand, the CB treated group indicated significant alterations in 17 metabolites compared to the model group and, the altered metabolites were involved in the four pathways, supporting the anti-obesity and lipid lowering effects of CB extract.

The TCA cycle is strongly associated with metabolic disorders such as obesity, insulin resistance and type 2 diabetes (Prentki & Madiraju, 2012). In the TCA cycle, acetyl-CoA has a notable role for FA biosynthesis, elongation, and fat synthesis (Martinez, Tsuchiya, & Gout, 2014; Hirokawa et al., 2020). FA synthesis is constituted through a major process of utilizing acetyl-CoA. The acetyl-CoA participates FA synthesis and oxidation as a precursor through transforming from acetyl-CoA to malonyl-CoA by acetyl-CoA carboxylase (Brownsey et al., 2006). Thus, to minimize FA biosynthesis and elongation, it is required the high usage of acetyl-CoA in energy metabolism such as TCA cycle.

The CB extract reversed the regulation of TCA cycle intermediates, implicating acceleration of glycolysis. The CB group restored the up-regulated pyruvate, pantothenate, glucose 6-phosphate, D-glucuronate, and other TCA cycle intermediates (Fig. 8). The up-regulated pyruvate can be converted by oxidation and decar-

boxylation to acetyl-CoA for TCA cycle. Also, pantothenic acid level in CB group was approximately two-fold enhanced compared to the obese group. The pantothenic acid is a key substance for the synthesis of coenzyme A (CoA) by pantothenate kinases, transforming to acetyl-CoA (Martinez et al., 2014). Moreover, malate supplies oxaloacetate and NADH by mitochondrial malate dehydrogenase. Thus, the less malate causes the lower NADH production, which affects ATP generation (Hirokawa et al., 2020). The results suggested that the malate-oxaloacetate shuttle was weakened under HFHS diet and recovered by CB extracts. CB administration in obese rats increased the activities of main enzymes in TCA cycle such as hexokinase, glucose-6-phosphate dehydrogenase, and pyruvate kinase etc., which elevate energy metabolism. Consequently, CB extracts could have the effects of accelerating the metabolism of acetyl-CoA in the energy metabolism instead of FA synthesis and elongation.

There are several limitations to our study. First, this study confirmed the anti-obesity effects of CB extract on the morphology of adipose tissue by H&E staining, but we did not include the quantification of lipid droplets' accumulation. Second, CB extract accelerated the energy metabolism in obese rats, thus it is required to confirm if the energy expenditure is increased by CB administration in obese rats. Additionally, adipo-cytokines like adiponectin increases energy expenditure via activation of thermogenesis in adipose cells (Xu et al., 2020). Thus, it would be beneficial to evaluate the adipo-cytokines in the future work.

## 5. Conclusion

This study investigated the weight loss and lipid-lowering effect of CB on rats with HFHS diet-induced obesity through pharmaco-



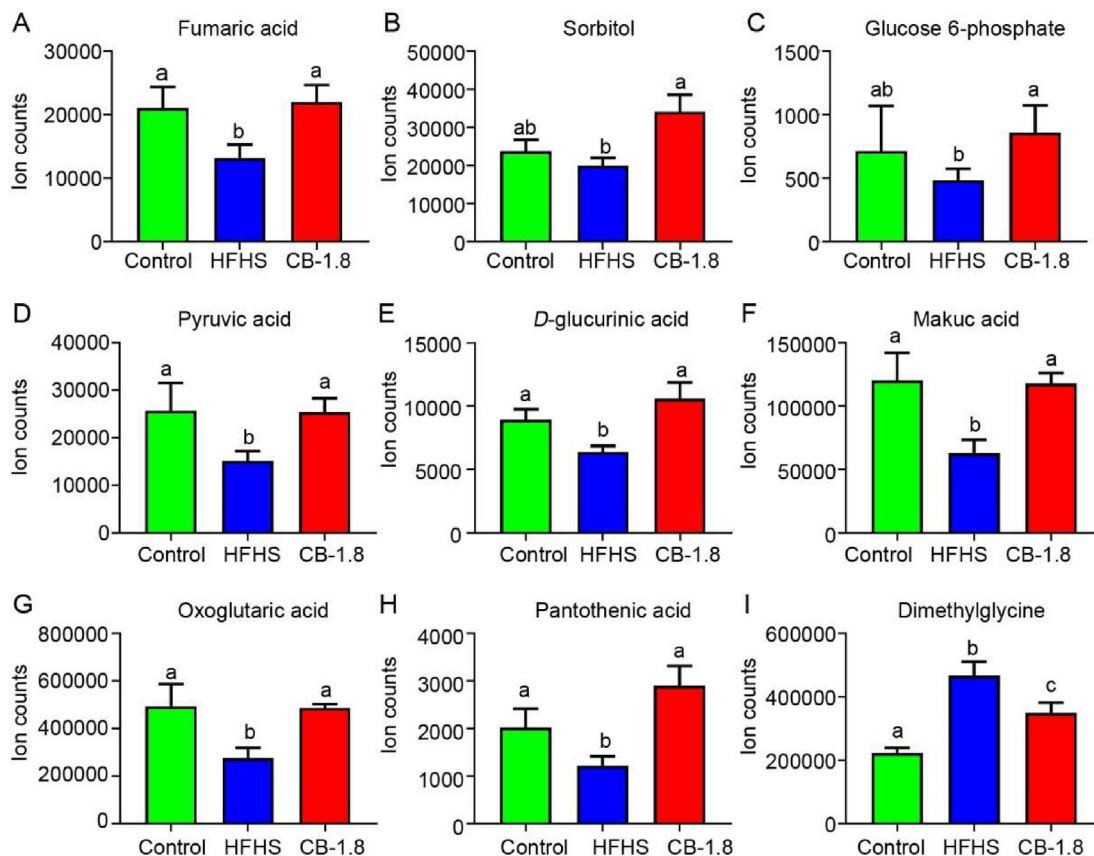


**Fig. 7.** Significantly differentiate expression of individual metabolites. A–I, Nine identified metabolites that differed significantly among control, HFHS, and CB-1.8 groups. The a, b, and c different letters indicated a significant difference at  $P < 0.05$ .

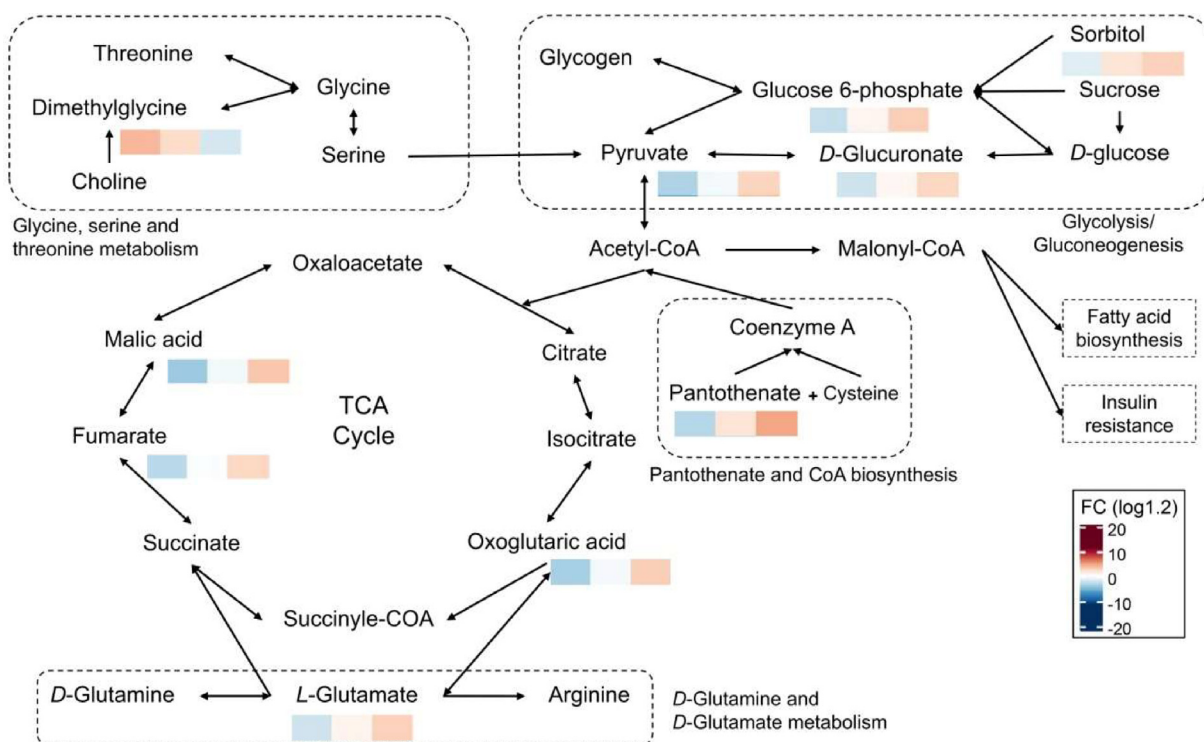


**Fig. 8.** Potential pathways related to the CB effect on HFHS diet-induced obese rats. The relative levels of critical metabolites were presented in color (blue—the lowest level; red—the highest level) following the control group, HFHS group, and CB-1.8 group.

logical evaluations and GC-TOF/MS metabolomics. The results of the performance, histological and biomedical assays, and metabolic alterations all demonstrated potential weight loss and lipid-lowering effects of CB. The metabolomics analysis revealed that CB extract restored the disturbing metabolic pathways, such as TCA cycle, lipid and glucose metabolism. Our study suggested nine metabolites as potential biomarkers for evaluating the mechanisms of weight loss and lipid-lowering effects of CB.

### Declaration of Competing Interest

The authors declare that they have no known competing financial interests or personal relationships that could have appeared to influence the work reported in this paper.

### Acknowledgements

This study was supported by China National Natural Science Foundation Project (No. 81803845), Inner Mongolia Autonomous Region Natural Science Foundation Project (No. 2018MS08040), “Mongolian Medicine Food and Drug Source Protection and Utilization Innovation Team” Construction Project (No. 190301), Mongolian Medicine Standardization Research International Cooperation Science and Technology Innovation project (No. MDKBZH2018009), Open Project of Key Laboratory of Mongolian Medicine Research and Development project of Ministry of Education (No. MDK2018056).

### Appendix A. Supplementary data

Supplementary data to this article can be found online at <https://doi.org/10.1016/j.chmed.2022.04.001>.

### References

- Amor, S., González-Hedström, D., Martín-Carro, B., Inarejos-García, A. M., Almodóvar, P., Prodanov, M., ... Granado, M. (2019). Beneficial effects of an aged black garlic extract in the metabolic and vascular alterations induced by a high fat/sucrose diet in male rats. *Nutrients*, *11*(1), 153.
- Aung, K. K., Lorenzo, C., Hinojosa, M. A., & Haffner, S. M. (2014). Risk of developing diabetes and cardiovascular disease in metabolically unhealthy normal-weight and metabolically healthy obese individuals. *Journal of Clinical Endocrinology and Metabolism*, *99*, 462–468.
- Ba, D. R. H., & Li, J. (2012). *Encyclopedia of Mongolian Studies: Medical Science* (1st ed., pp. 253–254). Huhhot: IM People's Publishing House.
- Bao, L., Gao, H., Zheng, Z., Zhao, X., Zhang, M., Jiao, F., ... Qian, Y. (2020). *Morus atropurpurea* integrated transcriptomic and un-targeted metabolomics analysis reveals mulberry fruit (*Morus atropurpurea*) in response to Sclerotinia pathogen infection. *International Journal of Molecular Sciences*, *21*, 1–18.
- Bessesen, D. H., & Van, G. L. F. (2018). Progress and challenges in anti-obesity pharmacotherapy. *The Lancet Diabetes & Endocrinology*, *6*, 237–248.
- Brownsey, R. W., Boone, A. N., Elliott, J. E., Kulpa, J. E., & Lee, W. M. (2006). Regulation of acetyl-CoA carboxylase. *Biochemical Society Transactions*, *34*, 223–227.
- Cataldi, M., Muscogiuri, G., Savastano, S., Barrea, L., Guida, B., Tagliabene, M., & Colao, A. (2019). Gender-related issues in the pharmacology of new anti-obesity drugs. *Obesity Reviews*, *20*, 1–10.
- Dangol, M., Kim, S. Y., Li, C. G., Fakhraei, L. S., Jang, M. Y., Ma, Y. H., ... Jung, H. (2017). Anti-obesity effect of a novel caffeine-loaded dissolving microneedle patch in high-fat diet-induced obese C57BL/6j mice. *Journal of Controlled Release*, *265*, 41–47.
- Darcy, J., Fang, Y., McFadden, S., Lynes, M. D., Leiria, L. O., & Dreyfuss, J. M. (2020). Integrated metabolomics reveals altered lipid metabolism in adipose tissue in a model of extreme longevity. *GeroScience*, *42*, 1–20.
- Deng, Y. J., Zhang, Y. P., Yang, Q. H., Han, L., Liang, Y. J., He, Y. F., ... Zhang, J. W. (2016). Effects of berberine on hepatic sirtuin 1-uncoupling protein 2 pathway in non-alcoholic fatty liver disease rats induced by high-fat diet. *Chinese Herbal Medicines*, *8*(4), 359–365.
- Dong, Z. B., Zhang, Y. H., Zhao, B. J., Li, C., Tian, G., Niu, B., ... Shao, J. G. (2015). Screening for anti-inflammatory components from *Corydalis bungeana* Turcz. based on macrophage binding combined with HPLC. *BMC Complementary and Alternative Medicine*, *15*, 1–10.
- Dong, H., Yan, G., Wang, Z., Wu, C., Cui, B., Ren, Y., & Yang, C. (2018). Liquid chromatography-tandem mass spectrometry simultaneous determination and pharmacokinetic study of fourteen alkaloid components in dog plasma after oral administration of *Corydalis bungeana* Turcz extract. *Molecules*, *23*, 1927.
- Hirokawa, Y., Kubo, T., Soma, Y., Saruta, F., & Hanai, T. (2020). Enhancement of acetyl-CoA flux for photosynthetic chemical production by pyruvate dehydrogenase complex overexpression in *Synechococcus elongatus* PCC 7942. *Metabolic Engineering*, *57*, 23–30.
- Hu, Y., Zhang, Y., Liu, C., Qin, R., Gong, D., & Wang, R. (2020). Multi-omics profiling highlights lipid metabolism alterations in pigs fed low-dose antibiotics. *BMC Genetics*, *21*, 1–12.
- Liu, X., Yang, Z., Li, H., Luo, W., Duan, W., Zhang, J., & Zhu, Z. (2020). Chrysophanol alleviates metabolic syndrome by activating the SIRT6/AMPK signaling pathway in brown adipocytes. *Oxidative Medicine and Cellular Longevity*, *20*, 1–14.
- Martinez, D. L., Tsuchiya, Y., & Gout, I. (2014). Coenzyme A biosynthetic machinery in mammalian cells. *Biochemical Society Transactions*, *42*, 1112–1117.
- Mediani, A., Abas, F., Maulidiani, M., Sajak, A. B., Khatib, A., Tan, C. P., Ismail, I. S., Shaari, K., Ismail, A., & Lajis, N. H. (2018). Metabolomic analysis and biochemical changes in the urine and serum of streptozotocin-induced normal-and obese-diabetic rats. *Journal of Physiology Biochemistry*, *74*(3), 403–416.
- Mesnage, R., Biserini, M., Balu, S., Frainay, C., & Poupin, N. (2018). Integrated transcriptomics and metabolomics reveal signatures of lipid metabolism dysregulation in HepaRG liver cells exposed to PCB 126. *Archives of Toxicology*, *92*, 1533–1547.
- Mooradian, A. (2009). Dyslipidemia in type 2 diabetes mellitus. *Nature Clinical Practice Endocrinology & Metabolism*, *5*, 150–159.
- O'Neill, S., & O'Driscoll, L. (2015). Metabolic syndrome: A closer look at the growing epidemic and its associated pathologies. *Obesity Reviews*, *16*, 1–12.
- Prentki, M., & Madiraju, S. M. (2012). Glycerolipid/free fatty acid cycle and islet  $\beta$ -cell function in health, obesity and diabetes. *Molecular and Cellular Endocrinology*, *353*, 88–100.
- Shafaie, Y., Koelliker, Y., Hoffman, D. J., & Tepper, B. J. (2013). Energy intake and diet selection during buffet consumption in women classified by the 6-n-propylthiouracil bitter taste phenotype. *American Journal of Clinical Nutrition*, *98*, 1583–1591.
- Stanhope, K. L., Schwarz, J. M., Keim, N. L., Griffen, S. C., Bremer, A. A., & Graham, J. L. (2009). Consuming fructose-sweetened, not glucose-sweetened, beverages increases visceral adiposity and lipids and decreases insulin sensitivity in overweight/obese humans. *Journal of Clinical Investigation*, *119*, 1322–1334.
- Sumiyoshi, M., Sakanaka, M., & Kimura, Y. (2006). Chronic intake of high-fat and high-sucrose diets differentially affects glucose intolerance in mice. *Journal of Nutrition*, *136*, 582–587.
- Tang, Y., Zhang, Y., Wang, C., Sun, Z., Li, L., & Cheng, S. (2018). Overexpression of PCK1 gene antagonizes hepatocellular carcinoma through the activation of gluconeogenesis and suppression of glycolysis pathways. *Cellular Physiology and Biochemistry*, *47*, 344–355.
- Tian, M., Yang, C., Yang, J., Dong, H., Liu, L., Ren, Y., & Wang, Z. (2019). Ultrahigh performance liquid chromatography-electrospray ionization tandem mass spectrometry method for qualitative and quantitative analyses of constituents of *Corydalis bungeana* Turcz extract. *Molecules*, *24*, 3463.
- Venables, M. C., Hulston, C. J., Cox, H. R., & Jeukendrup, A. E. (2008). Green tea extract ingestion, fat oxidation, and glucose tolerance in healthy humans. *American Journal of Clinical Nutrition*, *87*, 778–784.
- Wang, Z. J., Bai, Z., Yan, J. H., Liu, T. T., Li, Y. M., Xu, J. H., ... Bi, Y. F. (2021). Anti-diabetic effects of linarin from *Chrysanthemi Indici Flos* via AMPK activation. *Chinese Herbal Medicines*, *14*(1), 97–103.
- Xu, X., Wang, W. T., Zhao, Z. Y., Xi, W. G., Yu, B., Hao, C. H., ... Tang, L. D. (2020). Effects of total iridoid glycosides of *Picrorhiza scrophulariiflora* against non-alcoholic steatohepatitis rats induced by high-fat and high-sugar diet through regulation of lipid metabolism. *Chinese Herbal Medicines*, *12*(01), 67–72.
- Yang, Z. H., Miyahara, H., Takeo, J., & Katayama, M. (2012). Diet high in fat and sucrose induces rapid onset of obesity-related metabolic syndrome partly through rapid response of genes involved in lipogenesis, insulin signalling and inflammation in mice. *Diabetology & Metabolic Syndrome*, *4*, 1–10.
- Yang, C., Zhang, C., Wang, Z., Tang, Z., Kuang, H., & Kong, A. N. (2016). Corynoline isolated from *Corydalis bungeana* Turcz. exhibits anti-inflammatory effects via modulation of Nfr2 and MAPKs. *Molecules*, *21*, 975.
- Zhai, X. T., Chen, J. Q., Jiang, C. H., Song, J., Li, D. Y., Zhang, H., ... Zhu, F. X. (2016). *Corydalis bungeana* Turcz. attenuates LPS-induced inflammatory responses via the suppression of NF- $\kappa$ B signaling pathway *in vitro* and *in vivo*. *Journal of Ethnopharmacology*, *194*, 1–29.
- Zhang, M., Lv, X. Y., Li, J., Xu, Z. G., & Chen, L. (2008). The characterization of high-fat diet and multiple low-dose streptozotocin induced type 2 diabetes rat model. *Experimental Diabetes Research*, *1*–10.